Thermodynamically self-consistent theory for the Blume-Capel model

S. Grollau, E. Kierlik, M. L. Rosinberg, and G. Tarjus
Laboratoire de Physique Théorique des Liquides, Université Pierre et Marie Curie, 4 Place Jussieu, 75252 Paris Cedex 05, France*
(Received 21 July 2000; published 27 March 2001)

We use a self-consistent Ornstein-Zernike approximation to study the Blume-Capel ferromagnet on three-dimensional lattices. The correlation functions and the thermodynamics are obtained from the solution of two coupled partial differential equations. The theory provides a comprehensive and accurate description of the phase diagram in all regions, including the wing boundaries in a nonzero magnetic field. In particular, the coordinates of the tricritical point are in very good agreement with the best estimates from simulation or series expansion. Numerical and analytical analysis strongly suggest that the theory predicts a universal Ising-like critical behavior along the λ line and the wing critical lines, and a tricritical behavior governed by mean-field exponents.

DOI: 10.1103/PhysRevE.63.041111 PACS number(s): 05.20.Gg, 64.60.−i, 05.50.+q

I. INTRODUCTION

The self-consistent Ornstein-Zernike approximation (SCOZA) has been introduced some time ago by Hoye and Stell [1] as a method for obtaining thermodynamic and structural properties of simple fluid and lattice-gas systems. Like the mean-spherical approximation, this approach is based on the assumption that the direct correlation function $C(\mathbf{r})$, which is related to the two-particle distribution function $G(\mathbf{r})$ via the Ornstein-Zernike (OZ) equation, is proportional to the pair potential outside the hard-core region (or, for a lattice gas, for $\mathbf{r}\neq\mathbf{0}$). But the dependence of the proportionality constant on density and temperature is determined in such a way that the same free energy is obtained from fluctuation theory—the so-called compressibility or susceptibility route—and from integration of the internal energy with respect to the inverse temperature. For the lattice gas with nearest-neighbor attractive interactions (or equivalently, for the ferromagnetic spin-$\frac{1}{2}$ Ising model), this thermodynamic self-consistency is embodied in a partial differential equation whose solution, along with the requirement of single site occupancy, fixes $C(\mathbf{r})$ [and thus $G(\mathbf{r})$] uniquely. Because of numerical difficulties, this equation was only solved recently [2], showing that the SCOZA provides an accurate description of the properties of the three-dimensional (3D) Ising model over most of the phase diagram. The predicted values of T_c for the various cubic lattices are within 0.2% of their best estimates, the effective critical exponents are faithful to the true behavior above T_c except in a very narrow neighborhood of the critical point, and the zero-field magnetization is described asymptotically by the nonclassical exponent $\beta=0.35$ [3]. The SCOZA has been also extended to n component and continuous spins [4], and accurate results have been obtained for the hard-core Yukawa fluid [5] and for several spin systems in the presence of quenched disorder [6].

The purpose of this paper is to apply the same type of approximation to the Blume-Capel model [7], a special case of the spin-1 Blume-Emery-Griffiths (BEG) model [8], which represents a variety of interesting physical systems, in particular ^{3}He-^{4}He mixtures. This model has played an important role in the development of the theory of tricritical phenomena [9,10] and has been very actively studied over the years, following the original mean-field treatment of BEG [8]. Various methods like series expansions [11], renormalization-group calculations [12], and Monte Carlo simulations [13] have been used to describe the first- and second-order regions, the tricritical region, and the crossover between them. A study of the coexistence curve using the mean-spherical approximation has also been proposed recently [14]. There is no analytical theory, however, which is able to provide a comprehensive and accurate description of the phase diagram in all regions (including the ''wing'' boundaries in a nonzero magnetic field). As we shall see in the following, the SCOZA reaches this goal quite successfully without requiring prohibitive computational effort. In particular, the coordinates of the tricritical point (TCP) for the various cubic lattices are predicted with very good accuracy and the universal asymptotic tricritical behavior is well described. This suggests that the SCOZA is a reliable theory for exploring three-dimensional systems that exhibit first order as well as continuous transitions.

The paper is organized as follows: in Sec. II we describe the theory and derive the partial differential equations that encode the thermodynamics of the model, in Sec. III we present our results for the phase diagram, and in Sec. IV we discuss the universal properties in the second-order and tricritical regions. Our conclusions are drawn in Sec. V. The extension of the theory to the full spin-1 Hamiltonian is presented in Appendix A and details on the scaling behavior near the TCP are reported in Appendix B.

II. THEORY

The Blume-Capel (BC) model [7] is defined by the Hamiltonian

$$\mathcal{H}_{BC}=-J\sum_{\langle ij\rangle} S_iS_j+\Delta\sum_i S_i^2-h\sum_i S_i, \qquad (1)$$

*The Laboratoire de Physique Théorique des Liquides is the UMR 7600 of the CNRS.

where $S_i=0,\pm 1$ is the spin variable at each site i of a d-dimensional lattice and the first term sums over all nearest-neighbor (n.n.) pairs. This is a special case of the BEG Hamiltonian [8], $\mathcal{H}_{BEG}=\mathcal{H}_{BC}-K\Sigma_{\langle ij\rangle}S_i^2S_j^2$, which is a microscopic model for ^{3}He-^{4}He mixtures. $S_i=0$ represents a ^{3}He atom at site i and $S_i=\pm 1$ a ^{4}He atom, with the sign in the latter case describing the superfluid degree of freedom. In this interpretation, the coupling constant $J>0$ is a potential that promotes superfluidity, the crystal field Δ reflects the chemical-potential difference between the isotopes, and K represents the difference in the van der Waals interactions between the isotopes (the actual value of K/J is small, so that setting $K=0$ is a sensible approximation). The magnetization $m=\langle S_i\rangle$ identifies to the superfluid order parameter and $x=1-\langle S_i^2\rangle$ represents the ^{3}He concentration. As is well known, the phase diagram of ^{3}He-^{4}He mixtures presents a line of second-order transitions (the so-called λ line) at high temperatures and high ^{4}He concentrations and a coexistence region associated with a first-order transition at low temperatures. The BC Hamiltonian may also describe a spin-$\frac{1}{2}$ Ising model with a fractional concentration x of nonmagnetic impurities in thermal equilibrium with the spin system (annealed dilution). Δ is then interpreted as the chemical potential that controls the impurity concentration (the case of quenched dilution has been studied in Ref. [6]).

Our theory for the Blume-Capel model is based on an Ornstein-Zernike approximation for the direct correlation function C_{ij}, which is the inverse of the connected pair correlation function $G_{ij}=\langle S_iS_j\rangle-\langle S_i\rangle\langle S_j\rangle$, i.e.,

$$\sum_k G_{ik}C_{kj}=\delta_{ij}, \tag{2}$$

where δ_{ij} is the Kronecker symbol. This OZ equation may be considered as the definition of C_{ij}. It is also a consequence of the Legendre transform

$$\mathcal{G}=\mathcal{F}+\sum_i h_im_i \tag{3}$$

that defines the Gibbs free energy $\mathcal{G}$ from the free energy $\mathcal{F}=-k_BT\ln \mathrm{Tr}\exp[-\mathcal{H}_{BC}/(k_BT)]$. In Eq. (3), a site-dependent magnetic field h_i has been introduced for convenience and $\langle S_i\rangle=-\partial\mathcal{F}/\partial h_i=m_i$ is the local magnetization. The second functional derivatives of $\mathcal{F}$ and $\mathcal{G}$ with respect to the local fields and local magnetizations generate G_{ij} and C_{ij}, respectively,

$$G_{ij}=-\frac{\partial^2\tilde{\mathcal{F}}}{\partial\tilde{h}_i\partial\tilde{h}_j}, \tag{4}$$

$$C_{ij}=\frac{\partial^2\tilde{\mathcal{G}}}{\partial m_i\partial m_j}, \tag{5}$$

where $\tilde{\mathcal{F}}=\beta\mathcal{F},\tilde{\mathcal{G}}=\beta\mathcal{G}$, and $\tilde{h}_i=\beta h_i$ [$\beta=(k_BT)^{-1}$ is the inverse temperature]. For a uniform magnetic field $h_i=h$, the system is translationally invariant and the correlation functions only depend on the vector $\mathbf{r}$ that connects the two sites. The OZ equation then simplifies to

$$\hat{C}(\mathbf{k})\hat{G}(\mathbf{k})=1 \tag{6}$$

in Fourier space.

In contrast with $G(\mathbf{r})$, the direct correlation function is expected to remain a short-ranged function even in the critical region [specifically, $\hat{C}(\mathbf{k}=\mathbf{0})<+\infty$]. In the following, we shall assume that $C(\mathbf{r})$ has always the same range as the pair potential. This OZ ansatz is the *only* approximation in our theory. Since the exchange interaction in the Blume-Capel Hamiltonian is limited to nearest-neighbor (nn) sites, this amounts to setting

$$C(\mathbf{r})=c_0(\tilde{J},\tilde{\Delta},m)\,\delta_{\mathbf{r},0}+c_1(\tilde{J},\tilde{\Delta},m)\,\delta_{\mathbf{r},\mathbf{e}} \tag{7}$$

or in Fourier space,

$$\hat{C}(\mathbf{k})=c_0(\tilde{J},\tilde{\Delta},m)[1-z(\tilde{J},\tilde{\Delta},m)\hat{\lambda}(\mathbf{k})], \tag{8}$$

where $\mathbf{e}$ is a vector from the origin to one of its nearest neighbors, $\hat{\lambda}(\mathbf{k})=(1/c)\Sigma_{\mathbf{e}}e^{i\mathbf{k}.\mathbf{e}}$ is the characteristic function of the lattice (c is the coordination number), and $z=-(c_1/c_0)c$. c_0 and c_1 (or, equivalently, c_0 and z) are functions of $\tilde{J}=\beta J,\tilde{\Delta}=\beta\Delta$, and m, which will be obtained below from the solution of the SCOZA partial differential equations (in the simpler mean-spherical approximation studied in Ref. [14], one has just $c_1=-\tilde{J}$). It is worth noticing that the range of $C(\mathbf{r})$ is exactly limited to n.n. separation in one dimension. This can be easily checked by using the transfer-matrix method (see, e.g., Ref. [15]) to calculate $G(\mathbf{r})$ and then inverting the OZ equation to get the direct correlation function (this result holds for the most general spin-1 Hamiltonian with nn pair interactions $\mathcal{H}=\mathcal{H}_{BC}-K\Sigma_{\langle ij\rangle}S_i^2S_j^2-L\Sigma_{\langle ij\rangle}S_iS_j(S_i+S_j)$, which is used as a model for ternary mixtures [16]). $C(\mathbf{r})$ has the same spatial structure in the limit of infinite dimension (where the mean-field approximation becomes exact), and we expect that Eq. (8) is a reasonable assumption for $d=3$. A major consequence is that $G(\mathbf{r})$ is given in any dimension by

$$G(\mathbf{r})=\frac{1}{c_0}P(\mathbf{r},z), \tag{9}$$

where

$$P(\mathbf{r},z)=\frac{1}{(2\pi)^d}\int_{-\pi}^{\pi}d\mathbf{k}\frac{e^{-i\mathbf{k}.\mathbf{r}}}{1-z\hat{\lambda}(\mathbf{k})} \tag{10}$$

is the lattice Green's function [for instance, $\hat{\lambda}(\mathbf{k})=\frac{1}{3}(\cos k_x+\cos k_y+\cos k_z)$ for the simple cubic lattice]. The variable z (with $0\leqslant z\leqslant 1$) is related to the second-moment correlation length ξ defined by $\hat{G}(\mathbf{k})\sim\hat{G}(\mathbf{0})(1+\xi^2k^2)$, $k\to 0$, where $\beta\hat{G}(\mathbf{0})\equiv\partial m/\partial h=\beta/[c_0(1-z)]$. Specifically, one has $2d\xi^2=z/(1-z)$ for the simple hypercubic lattice. Therefore, for a given value of the crystal-field $\tilde{\Delta}$, the condition $z=1$ gives the locus of diverging correlation length and diverging sus-

ceptibility in the $(\tilde{J},m)$ plane. This defines a spinodal surface in the $(\tilde{J},\tilde{\Delta},m)$ space; in particular, $z(\tilde{J},\tilde{\Delta},m=0)=1$ corresponds to the λ line in the region of the $h=0$ phase diagram where the transition is continuous.

In order to determine the two unknown functions c_0 and z, we impose thermodynamic self-consistency. To this end, we consider the change in the free energy associated with infinitesimal changes in $\tilde{J},\tilde{\Delta}$ and $\tilde{h}$:

$$\delta\tilde{\mathcal{F}}=-\delta\tilde{J}\sum_{\langle ij\rangle}\langle S_iS_j\rangle+\delta\tilde{\Delta}\sum_i\langle S_i^2\rangle-\delta\tilde{h}\sum_i\langle S_i\rangle. \quad (11)$$

In terms of the pair-correlation function, this gives

$$\delta\tilde{\mathcal{F}}/N=-\frac{1}{2}[G(\mathbf{r}=\mathbf{e})+m^2]\delta\lambda+[G(\mathbf{r}=\mathbf{0})+m^2]\delta\tilde{\Delta}-m\,\delta\tilde{h}, \quad (12)$$

where N is the number of lattice sites and the coordination number c has been absorbed in the new inverse temperature variable $\lambda=c\tilde{J}$. The corresponding change in the Gibbs free energy is

$$\delta\tilde{\mathcal{G}}/N=-\frac{1}{2}[G(\mathbf{r}=\mathbf{e})+m^2]\delta\lambda+[G(\mathbf{r}=\mathbf{0})+m^2]\delta\tilde{\Delta}+\tilde{h}\,\delta m. \quad (13)$$

On the other hand, from Eq. (5), we have

$$\frac{\partial^2\tilde{\mathcal{G}}/N}{\partial m^2}=\hat{C}(\mathbf{k}=\mathbf{0}). \quad (14)$$

Therefore, in order to get the same Gibbs free energy when integrating with respect to $\lambda,\tilde{\Delta}$, or m, the following Maxwell relations must be satisfied:

$$\frac{\partial\hat{C}(\mathbf{k}=\mathbf{0})}{\partial\lambda}=-\frac{1}{2}\frac{\partial^2}{\partial m^2}[G(\mathbf{r}=\mathbf{e})+m^2], \quad (15a)$$

$$\frac{\partial G(\mathbf{r}=\mathbf{0})}{\partial\lambda}=-\frac{1}{2}\frac{\partial G(\mathbf{r}=\mathbf{e})}{\partial\tilde{\Delta}}, \quad (15b)$$

$$\frac{\partial\hat{C}(\mathbf{k}=\mathbf{0})}{\partial\tilde{\Delta}}=\frac{\partial^2}{\partial m^2}[G(\mathbf{r}=\mathbf{0})+m^2]. \quad (15c)$$

Clearly, only two of these equations are independent and in the following we shall use Eqs. (15a) and (15b).

Replacing $\tilde{\Delta}$ by the new variable $\tau=(1+\frac{1}{2}e^{\tilde{\Delta}})^{-1}$ which varies from 0 to 1, and inserting the explicit expressions of $\hat{C}(\mathbf{k})$ at $\mathbf{k}=\mathbf{0}$, and $G(\mathbf{r})$ at $\mathbf{r}=\mathbf{0}$ and $\mathbf{r}=\mathbf{e}$ that are obtained from Eqs. (8)–(10), we finally get the two SCOZA equations,

$$\frac{\partial}{\partial\lambda}c_0(1-z)=-1-\frac{1}{2}\frac{\partial^2}{\partial m^2}\frac{P(z)-1}{zc_0}, \quad (16a)$$

$$\frac{\partial}{\partial\lambda}\frac{P(z)}{c_0}=\frac{1}{2}\tau(1-\tau)\frac{\partial}{\partial\tau}\frac{P(z)-1}{zc_0}, \quad (16b)$$

where $P(z)\equiv P(\mathbf{r}=\mathbf{0},z)$ and the relation $P(\mathbf{r}=\mathbf{e},z)=(P(z)-1)/z$ has been used. Given the appropriate boundary conditions, integration of these coupled partial differential equations (PDE) in the two unknown functions $c_0(\lambda,\tau,m)$ and $z(\lambda,\tau,m)$ gives at once the thermodynamics of the Blume-Capel model in the whole parameter space. Indeed, according to Eq. (13), the Gibbs free energy $\tilde{\mathcal{G}}(\lambda,\tau,m)$ can be obtained in the same run of integration from the integral of $-\frac{1}{2}[G(\mathbf{r}=\mathbf{e})+m^2]$ with respect to λ (thanks to the thermodynamic consistency, this is equivalent to integration with respect to $\tilde{\Delta}$ or to m). At fixed λ and τ, $\tilde{\mathcal{G}}$ as a function of m has the same shape as in mean-field theory [8], except that the unstable region inside the spinodal is excluded. At the critical temperature, there is a single minimum at $m=0$ for $\tau>\tau_t$ or three minima at 0 and $\pm\Delta m$ [with $\tilde{\mathcal{G}}(\pm\Delta m)=\tilde{\mathcal{G}}(0)$] for $\tau<\tau_t$. This defines the second- and first-order parts of the $h=0$ phase diagram, respectively. The maxima of the spinodal curves in the $T-m$ plane (corresponding to $\partial^2\mathcal{G}/\partial m^2=0$) define the lines of second-order critical points, i.e., the λ line for $\tau>\tau_t$ $(m=0)$ and the wing critical lines for $\tau<\tau_t$ $[m=\pm m_c(\tau)]$. In the latter case, the corresponding critical field is given by $\pm h_c=\partial(\mathcal{G}/N)/\partial m|_{m=\pm m_c}$. The coordinates (T_t,τ_t) of the TCP can be determined accurately by observing the change in the convexity of the spinodal at $m=0$.

From a computational point of view, the coupled PDE's, Eqs. (16), define an initial value problem. The inverse temperature variable λ plays the role of time and the equations describe how $z(\lambda,\tau,m)$ and $c_0(\lambda,\tau,m)$ propagate forward in time. We thus need to specify the initial condition at $\lambda=0$ and the boundary conditions at $\tau=1$, $\tau=0$, and $m=\pm1$ (actually, because of symmetry, one can restrict the domain of integration to $m\geqslant0$).

The initial condition $J=\lambda=0$ corresponds to the high-temperature limit where the spins are independent. The properties of the system can be calculated exactly and the correlation functions are nonzero only at $\mathbf{r}=\mathbf{0}$. This implies that $z=0$ and $\hat{C}(\mathbf{0})\equiv\partial\tilde{h}/\partial m=c_0$. The inverse susceptibility is readily obtained from the expression of the magnetization

$$m=\frac{e^{\tilde{h}}-e^{-\tilde{h}}}{e^{\tilde{\Delta}}+e^{\tilde{h}}+e^{-\tilde{h}}}, \quad (17)$$

which yields

$$c_0=\frac{[1-\tau+(m^2-2m^2\tau+\tau^2)^{1/2}]^2}{(1-m^2)[(1-\tau)(m^2-2m^2\tau+\tau^2)^{1/2}+(m^2-2m^2\tau+\tau^2)]}. \tag{18}$$

The boundary condition at $\tau=1$ is given by the solution of the SCOZA equation for the spin-$\frac{1}{2}$ Ising model. Indeed, this limit is reached when $\tilde{\Delta}\to-\infty$, and the $S=0$ state is thus completely suppressed. Equation (16b) then shows that $P(z)/c_0=f(m)$ and setting $\tau=1$ in Eq. (18) gives $f(m)=1-m^2$. The equation for the remaining variable $z(\lambda,m)$, Eq. (16a), becomes

$$\frac{1}{1-m^2}\frac{\partial}{\partial\lambda}(1-z)P(z)=-1-\frac{1}{2}\frac{\partial^2}{\partial m^2}\left[(1-m^2)\frac{P(z)-1}{zP(z)}\right], \tag{19}$$

which is the SCOZA equation for the Ising model studied in Ref. [2] (with the standard replacement of lattice-gas variables by spin variables). In Ref. [2], the unknown function c_0 was determined by using the hard-spin condition $S_i^2=1$, which implies that $G(\mathbf{r}=\mathbf{0})=P(z)/c_0=1-m^2$ (in lattice-gas language, this is the so-called *core* condition). Since the self-consistency conditions, Eqs. (15), are exact, it is not surprising that the same result comes out from our equations when the state $S=0$ is suppressed.

The second boundary at $\tau=0$ is reached when $\tilde{\Delta}\to+\infty$. The $S=\pm1$ states are then suppressed. This only happens, however, if the magnetic field h is finite. For $h\to\pm\infty$, one can still have a nonzero magnetization. As a consequence, z remains a nontrivial function of temperature and magnetization. The solution of Eqs. (16b) is again $P(z)/c_0=f(m)$, and setting $\tau=0$ in Eq. (18) gives $f(m)=m(1-m)$ for $m\geqslant0$. This leads to the equation

$$\frac{1}{m(1-m)}\frac{\partial}{\partial\lambda}(1-z)P(z)=-1-\frac{1}{2}\frac{\partial^2}{\partial m^2}\times\left[m(1-m)\frac{P(z)-1}{zP(z)}\right], \tag{20}$$

which identifies to Eq. (19) by replacing m by $(1-m)/2$ and λ by 4λ. Therefore, remarkably, the spinodal for $h\to\pm\infty$ can be deduced from the spinodal of the spin-$\frac{1}{2}$ Ising model. The two maxima at $m_c=\pm\frac{1}{2}$ and $T_c=\frac{1}{4}T_c^{Ising}$ correspond to second-order transitions that mark the end of the wing critical lines for $h_c\to\pm\infty$, as illustrated below.

Finally, the boundary $m=1$ is reached when all spins are in the $S=1$ state. Since there are no more fluctuations, one has $\xi=0$ and thus $z=0$, whereas $G(\mathbf{r}=\mathbf{0})=\langle S_i^2\rangle-\langle S_i\rangle^2=P(z)/c_0=0$ implies that $c_0\to\infty$.

The numerical integration of the PDE's was performed by using a finite-difference scheme in which the three variables λ, τ, and m are discretized and the partial derivatives are approximated by finite-difference representations [17]. The first derivatives with respect to λ are used to update z and c_0 at the temperature step $n+1$ by evaluating the first and second derivatives with respect to τ and m at the step n. In principle, this is a straightforward procedure. There are, however, two difficulties. First, the region of integration is bounded by the spinodal surface, which is not known in advance. Second, there is a singular behavior as one approaches the spinodal. To see this, let us rewrite the PDE's using as unknown functions z and the new variable $v=P(z)/c_0$. We get

$$A(z,v)\frac{\partial v}{\partial\lambda}+B(z,v)\frac{\partial z}{\partial\lambda}=-1-\frac{1}{2}\frac{\partial^2}{\partial m^2}[\psi(z)v], \tag{21a}$$

$$\frac{\partial v}{\partial\lambda}=\frac{1}{2}\tau(1-\tau)\frac{\partial}{\partial\tau}[\psi(z)v], \tag{21b}$$

where $A(z,v)=-P(z)(1-z)/v^2$, $B(z,v)=(1/v)\partial[(1-z)P(z)]/\partial z$ and $\psi(z)=[P(z)-1]/[zP(z)]$. Eq. (21a) can be viewed as a nonlinear diffusion equation and A^{-1} plays the role of a diffusion coefficient that diverges like $(1-z)^{-1}$ when $z\to1$, namely, on the spinodal surface. These two difficulties are already present in the equation for the Ising model, Eq. (19), but then the spinodal is just a line in the (λ,m) plane [2].

We solved the first problem as follows. Whenever the variable $z_n(\tau,m)$ at the temperature step n enters the interval $(1-\epsilon,1)$, where ϵ is small number (typically, $\epsilon\leqslant10^{-5}-10^{-6}$), we consider that the spinodal is reached and we stop the calculation. The spinodal is then defined by the corresponding values of τ and m. At the next temperature step, we use the same values z_n and v_n to compute the partial derivatives with respect to τ and m on the spinodal (in other words, we locally ''freeze'' the values of z and v inside the spinodal). On the other hand, the vanishingly small values of $A(z,v)$ for $z\to1$ impose a dramatic decrease of the inverse temperature spacing $\Delta\lambda$ as the spinodal is approached. Indeed, as is well known [17], solving a diffusion equation by an *explicit* method requires keeping the ''time'' step below a certain value that is proportional to D^{-1}, where D is the diffusion coefficient. In Ref. [2], this problem was avoided by using an *implicit* method, which is unconditionally stable. Unfortunately, it is not easy to generalize this procedure to a system of nonlinear PDE's like Eqs. (21) and we had to keep a simple explicit algorithm. In the high-temperature region, we typically adopted the spacings $\Delta m=\Delta\tau=10^{-2}$ and $\Delta\lambda=10^{-4}$. In the vicinity of the λ line and in the tricritical region, $\Delta\tau$ was set at 2.10^{-3} and $\Delta\lambda$ was gradually decreased down to 10^{-7}. This allowed to determine the critical parameters with excellent accuracy. For instance, in the limit $\tau\to1$, we found $\tilde{J}_c=0.221\,25$ for the inverse critical temperature of the Ising model on the simple cubic lattice. This corresponds to $\tilde{J}_c^{LG}=4\tilde{J}_c=0.88500$ for the n.n. lattice gas, in perfect agreement with the value obtained in Ref. [2] (this is

also within 0.2% of the best-estimate result [18]). When higher accuracy was required, for instance to determine the asymptotic critical exponents, $\Delta\lambda$ was further decreased to 10^{-9}. The integration was usually carried down to $k_BT/Jc \approx 0.18$ (below this value, the spinodal lines in the vicinity of $\tau=1$ are so close to the boundary $m=1$ that we could not integrate the equations with sufficient accuracy while keeping a reasonable spacing Δm; indeed, decreasing Δm forces also decreasing $\Delta\lambda$ in order to avoid numerical instabilities [17]).

Before presenting the numerical results, it is instructive to consider the high-temperature series expansion of the solution and compare it to the exact results. Since $z\to 0$ for $\lambda \to 0$, one can replace the Green's function $P(z)$ by its expansion in powers of z. We then expand z and c_0 as double series in λ and m^2, $z(\lambda,\tau,m)=\Sigma_{pq} z_{pq}(\tau)\lambda^p m^{2q}$ and $c_0(\lambda,\tau,m)=\Sigma_{pq} c^0_{pq}(\tau)\lambda^p m^{2q}$. The coefficients $z_{pq}(\tau)$ and $c^0_{pq}(\tau)$ are polynomials of τ that satisfy a system of linear algebraic equations at each order in λ and m^2. In the case of the fcc lattice ($c=12$, $P(z)=1+z^2/12+z^3/36+5z^4/192+5z^5/288+\ldots$) for which extensive series expansions have been derived by Saul *et al.* [11], the results for the zero-field ordering susceptibility $\chi_0=\Sigma_{\mathbf{r}} G(\mathbf{r};m=0)=\partial m/\partial h|_{h=0}$ and the second moment of the correlation function $\mu_2=\Sigma_{\mathbf{r}} r^2 G(\mathbf{r};m=0)=c\xi^2\chi_0$ are

$$k_BT\chi_0=\tau+12\tau^2\tilde{J}+6(\tau^2+21\tau^3)\tilde{J}^2+2(\tau^2+78\tau^3+621\tau^4)\tilde{J}^3+\frac{1}{2}(\tau^2+234\tau^3+5115\tau^4+23778\tau^5)\tilde{J}^4+\frac{1}{10}(\tau^2+612\tau^3+31851\tau^4+342\,690\tau^5+1\,122\,462\tau^6)\tilde{J}^5+\cdots \quad (22)$$

and

$$\mu_2=12\tau^2\tilde{J}+288\tau^3\tilde{J}^2+2(\tau^2+66\tau^3+2385\tau^4)\tilde{J}^3+\frac{1}{2}(240\tau^3+10080\tau^4+133\,488\tau^5)\tilde{J}^4+\frac{1}{10}\times(\tau^2+492\tau^3+50931\tau^4+1\,156\,410\tau^5+8\,474\,742\tau^6)\times\tilde{J}^5+\cdots. \quad (23)$$

Comparison with the exact series expansions shows that the coefficients in both expressions are exact through order $(\beta J)^4$ while higher-order terms do not deviate significantly from the exact ones. This is similar to the case of the spin-$\frac{1}{2}$ Ising model and we take this result as a strong indication that the numerical predictions of the SCOZA should be very close to the exact solution of the model.

To close this section, let us note that the present theory does not provide a *complete* description of the system. In particular, it does not give any information concerning the two correlation functions $G_{ij}^{S^2S^2}=\langle S_i^2S_j^2\rangle-\langle S_i^2\rangle\langle S_j^2\rangle$, and $G_{ij}^{SS^2}=\langle S_iS_j^2\rangle-\langle S_i\rangle\langle S_j^2\rangle$. In order to determine these functions, one needs to introduce a set of three different direct correlation functions. This implies to perform a double Legendre transform that defines a new Gibbs free energy, which is a function of m and x, the concentration order parameter, instead of m and Δ. The main interest of this alternative theory is that it allows to study the general spin-1 Hamiltonian with $K\neq 0$ and $L\neq 0$. On the other hand, the numerical solution is more difficult as one has to solve three coupled PDE's instead of two. Details on the derivation of these equations are given in Appendix A.

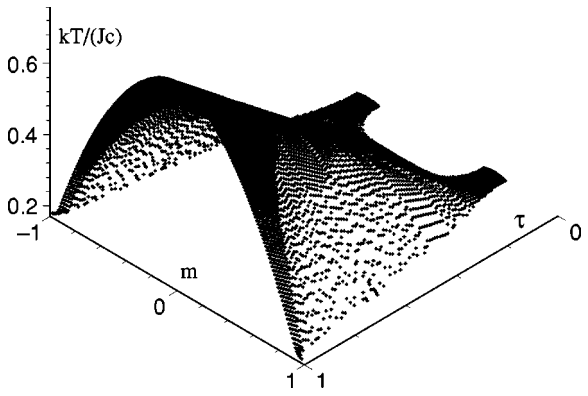

FIG. 1. SCOZA spinodal surface of the 3D Blume-Capel in the $(T-\tau-m)$ space.

III. RESULTS

In this section we concentrate on the SCOZA numerical predictions for the phase boundaries. These are nonuniversal properties that are lattice dependent. If not stated otherwise, the results presented here correspond to the simple cubic lattice for which no systematic study has been performed in the literature.

The overall shape of the spinodal surface in the (T,τ,m) space and the vicinity of the TCP are depicted in Figs. 1 and 2, respectively. We clearly see the evolution from the single curve at $\tau=1$ (the spinodal of the spin-$\frac{1}{2}$ model), which has a maximum at $m=0$ to the two symmetrical curves at $\tau=0$ with maxima located at $m_c=\pm\frac{1}{2}$, marking the end of the wing critical lines.

The $T_c(\tau)$, $T_c(\Delta)$, and $T_c(x)$ phase diagrams in zero field are shown in Figs. 3–5. Second- and first-order phase

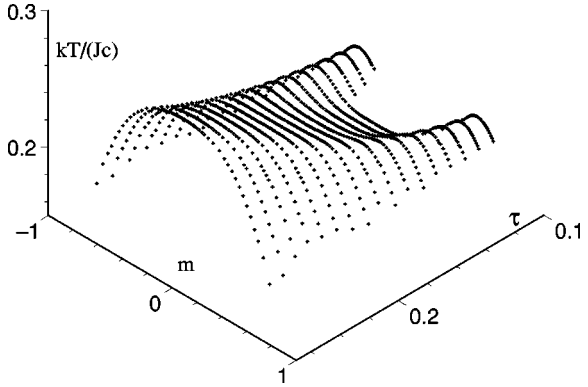

FIG. 2. Detail of the spinodal surface near the TCP.

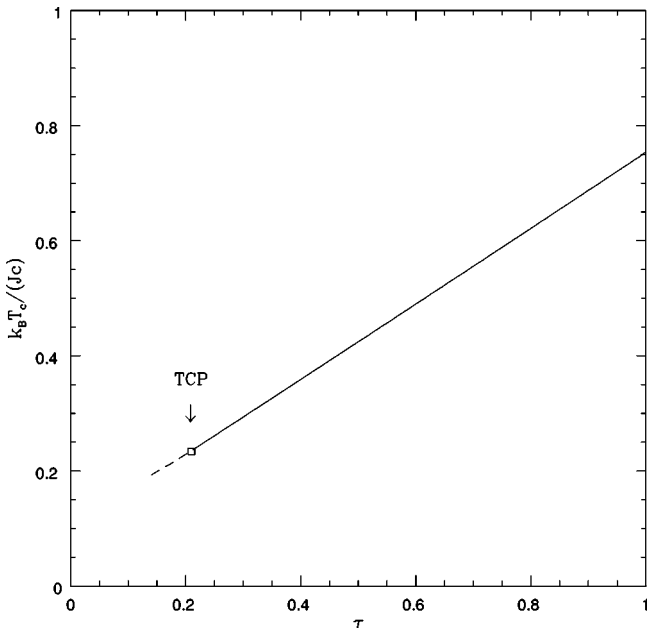

FIG. 3. Zero-field $T_c(\tau)$ phase diagram. Second-order and first-order parts of the phase boundary are shown as full and dashed lines, respectively. For numerical reasons, calculations have not been performed below $k_BT/(Jc)\approx 0.18$ (see text).

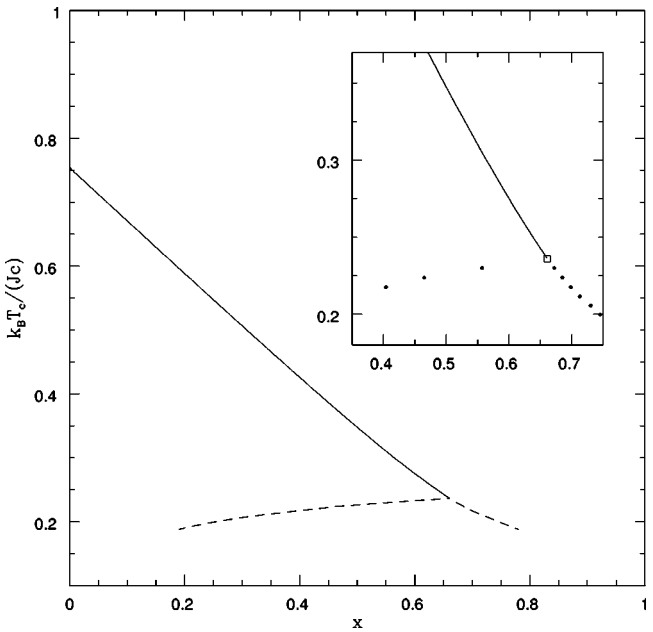

FIG. 5. Zero-field $T_c(x)$ phase diagram. Second-order and first-order parts of the phase boundary are shown as full and dashed lines, respectively. The inset describes the vicinity of the TCP.

boundaries are shown as full and dashed lines, respectively. The curves are quite similar to those obtained by series expansions [11] and Monte Carlo simulations [13] for the fcc lattice. In particular, we see that the slope of the phase boundary across the TCP is finite and continuous in both $T_c(\tau)$ and $T_c(\Delta)$ [specifically, we find $(T_t/Jc)\partial\Delta/\partial T|_{T_t}=-0.045$]; the $T_c(\Delta)$ phase boundary is slightly concave upward just below the TCP, and the λ line appears to extrapolate into the interior of the two-phase region in the $T_c(x)$ phase diagram (a continuous slope, however, cannot be strictly ruled out by our calculations). As is well known, the slope of the λ line and the slope of the coexistence curve on the ^{3}He-rich side are not the same experimentally. This is also predicted by renormalization-group analysis [9], in contrast with mean-field theory [8].

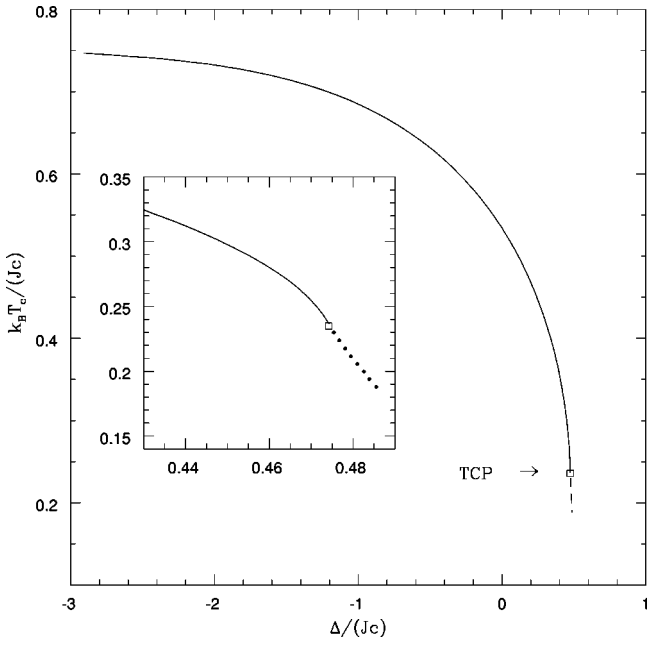

FIG. 4. Zero-field $T_c(\Delta)$ phase diagram. Second-order and first-order parts of the phase boundary are shown as full and dashed lines, respectively. The inset describes the vicinity of the TCP.

The accuracy of our calculation for the λ line in the Δ-T plane can be checked for the special value $\tilde{\Delta}=\ln 2$ for which a careful Monte Carlo calculation and finite-size study has been performed by Blöte *et al.* [18]. Our prediction for the inverse critical temperature $\tilde{J}_c=J/(k_BT_c)=0.3924$ is in excellent agreement their estimate $\tilde{J}_c=0.3934224(10)$. The accuracy of the theory is thus the same as for the spin-$\frac{1}{2}$ Ising model [2].

As noted earlier, the TCP corresponds to the point where the convexity of the spinodal in the T-τ plane changes at $m=0$. This is illustrated in Fig. 6, which shows the temperature dependence of the order parameter and the spinodal lines in the tricritical region on the first-order side of the phase boundary [observe that $\Delta m(\tau)$, the discontinuity in the order parameter across the first-order phase boundary, moves away from the spinodal as τ decreases]. The coordinates of the tricritical point are $k_BT_t/J=1.4160\pm 0.0040$, $\tau_t=0.2114\pm 0.0010$ $(\Delta_t/J=2.8457)$, $x_t=0.655\pm 0.006$, where the uncertainties reflect the finite size of the grid spacings. The predictions for T_t and Δ_t are in excellent agreement with the recent Monte Carlo estimates of Deserno [13]; $k_BT_t/J=1.4182\pm 0.0055$, $\Delta_t/J=2.8448\pm 0.0003$ (these numbers, however, are different from those quoted in Ref. [19], which locate the TCP near $k_BT_t/J=1.3900$, $\Delta_t/J=2.849$, and $x_t=0.61$; if these (unpublished) results are cor-

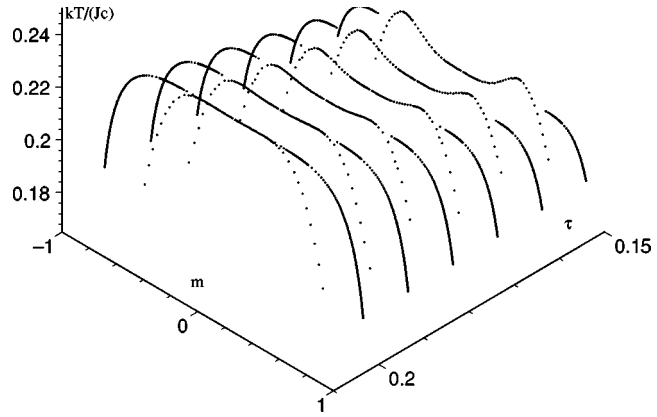

FIG. 6. Temperature dependence of the order parameter (full lines) and spinodal lines (dotted) in the vicinity of the TCP on the first-order part of the phase boundary.

rect, our value of x_t is overestimated and too close to the mean-field prediction, $x_t^{MF}=2/3$). Similarly, for the fcc lattice, we find $k_BT_t/J=3.1116\pm0.0090$, $\tau_t=0.2454\pm0.0010$ ($\Delta_t/J=5.6520$), and $x_t=0.658\pm0.006$, which we may compare with the Monte Carlo estimates of Jain and Landau [13] $k_BT_t/J=3.072\pm0.024$, $\Delta_t/J=5.652\pm0.048$, and $x_t=0.56\pm0.02$ (note that our value of x_t is in much better agreement with the series expansion estimate of Saul *et al.* [11], $x_t=0.665^{+0.005}_{-0.015}$; obviously, further work is needed to locate precisely the TCP in the $x-T$ plane). Finally, our predictions for the bcc lattice are $k_BT_t/J=2.0264\pm0.0060$, $\tau_t=0.2354\pm0.0010$ ($\Delta_t/J=3.7918$), and $x_t=0.656\pm0.006$ (to our knowledge, this lattice has only been studied by real-space renormalization-group methods [12] that do not predict accurately the location of the tricritical point).

At the TCP, the λ-line bifurcates into two symmetrical wing critical lines. The projections of the wing boundaries onto the $\Delta-T$, $\Delta-h$, and $T-h$ planes are shown in Fig. 7. Mean-field theory [8] predicts that the critical field h_c should go to infinity at $k_BT_c/Jc=\frac{1}{4}$. We clearly see in Fig. 7 that this value is overestimated. In fact, as noted earlier, the present theory predicts that $h_c\to\pm\infty$ at $k_BT_c/Jc=\frac{1}{4}k_BT_c^{Ising}/Jc=0.188$. For the fcc lattice, this yields $k_BT_c/Jc=0.204$, which is consistent with the value that can be extracted from the Monte Carlo simulations of Jain and Landau [13].

IV. ASYMPTOTIC BEHAVIOR IN THE CRITICAL AND TRICRITICAL REGIONS

As mentioned in the Introduction, the SCOZA for the 3D spin-$\frac{1}{2}$ Ising model has a nontrivial scaling behavior in the critical region [2,3]. Above T_c, the asymptotic behavior is the same as in the mean-spherical approximation and the exponents are those of the spherical model. This spherical scaling, however, is detectable only in a very narrow neighborhood of the critical point, and the effective SCOZA exponents are close to the true Ising ones down to reduced temperatures of around 10^{-2}. Below T_c, the scaling is neither spherical nor classical with two scaling functions instead of one [3]. Despite this shortcoming, the zero-field magnetization is very well described, with an asymptotic exponent $\beta=7/20=0.35$, which is close to the exact value $\beta\approx0.33$. It is thus interesting to also investigate the critical behavior of our SCOZA equations in the critical and tricritical regions of the 3D BC model.

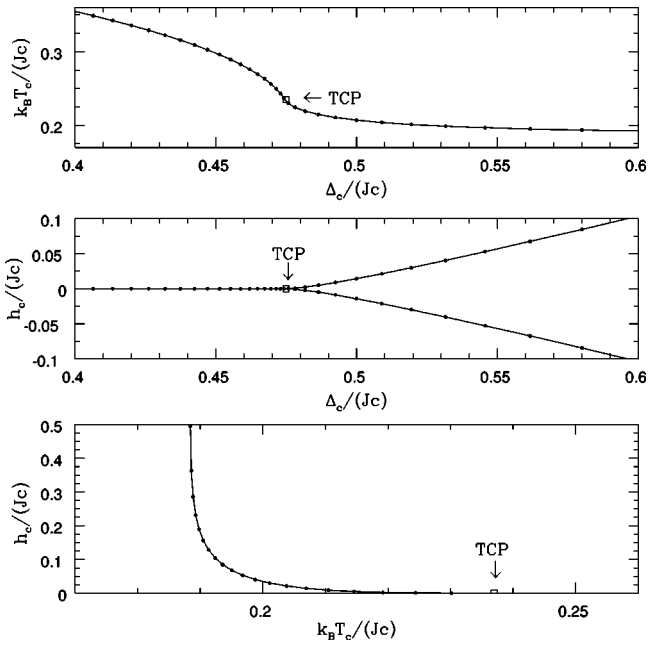

FIG. 7. Projections of the wing boundaries onto the $\Delta-T$, $\Delta-h$, and $T-h$ planes.

We first consider the behavior of the zero-field ordering susceptibility χ_0 as $T\to T_c(\tau)$ along paths of constant τ for $\tau\geqslant\tau_t$. Accurate evaluations were relatively straightforward to perform in the disordered phase: we only had to gradually decrease the spacing $\Delta\lambda$ as discussed earlier. Figure 8 shows a log-log plot of $k_BT\chi_0$ as a function of the reduced temperature $t=1-T_c/T$ together with the corresponding effective exponent γ_{eff} defined as the local slope $\partial\log(k_BT\chi_0)/\partial\log t$. In the region $1.0\geqslant\tau>0.25$, it can be seen that each $\gamma_{eff}(\tau)$ reaches the value 2 for $t\sim10^{-5}$ as in the case of the spin-$\frac{1}{2}$ model, showing that the asymptotic spherical behavior is universal. This is no more true when one moves further away from T_c. However, in the range $t\geqslant10^{-2}$, a quasiuniversal behavior is still observed for $1.0\geqslant\tau>0.6$, and the critical behavior is governed by an effective exponent that is close to the exact Ising value $\gamma\approx1.24$. On the other hand, as τ approaches its tricritical value $\tau_t=0.211$, there is an abrupt crossover to another behavior, which is governed by the exponent $\gamma_{eff}\approx1$ over a wide range of temperatures. There is good numerical evidence that γ_{eff} reaches 1 asymptotically at $\tau=\tau_t$.

For subcritical temperatures, it was more difficult to obtain accurate results in the vicinity of T_c because of our use of an explicit method to integrate the PDE's. Accordingly, we were only able to explore the critical behavior in a restricted range of temperatures $t=1-T/T_c$. Log-log plots of the temperature dependence of the order parameter m are shown in Figs. 9 and 10. Despite the limited range, it appears from Fig. 9 that in the second-order region well above the

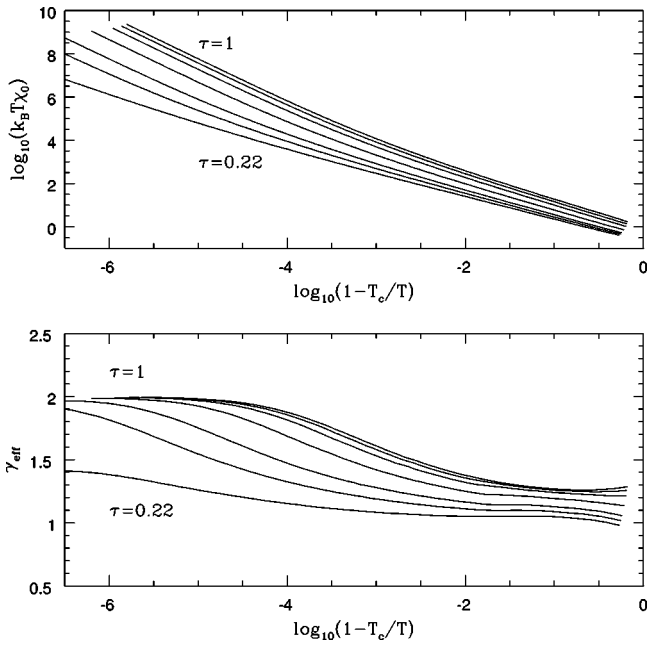

FIG. 8. Log-log plot of the zero-field ordering susceptibility $k_B T\chi_0$ as a function of the reduced temperature $1-T_c/T$ and corresponding effective exponent γ_{eff}. The different curves correspond to $\tau=1.00,\ 0.79,\ 0.60,\ 0.40,\ 0.29,\ \ 0.25$, and 0.22.

crossover to tricritical behavior, the slope of each curve has a common asymptotic limit that corresponds to the SCOZA prediction for the Ising model, $\beta_{scoza}^{Ising}=7/20$. Figure 10 shows that for smaller values of τ, one needs to go closer to T_c to reach this asymptotic universal regime. Again, we observe an abrupt crossover to another behavior as one enters the tricritical region. Our results are consistent with the

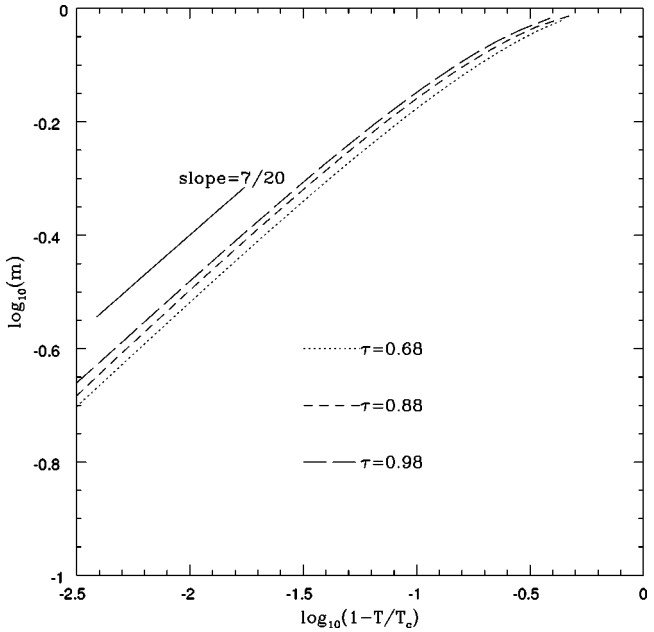

FIG. 9. Log-log plot of the order parameter m as a function of the reduced temperature $1-T/T_c$ in the second-order region well above the crossover to tricritical behavior.

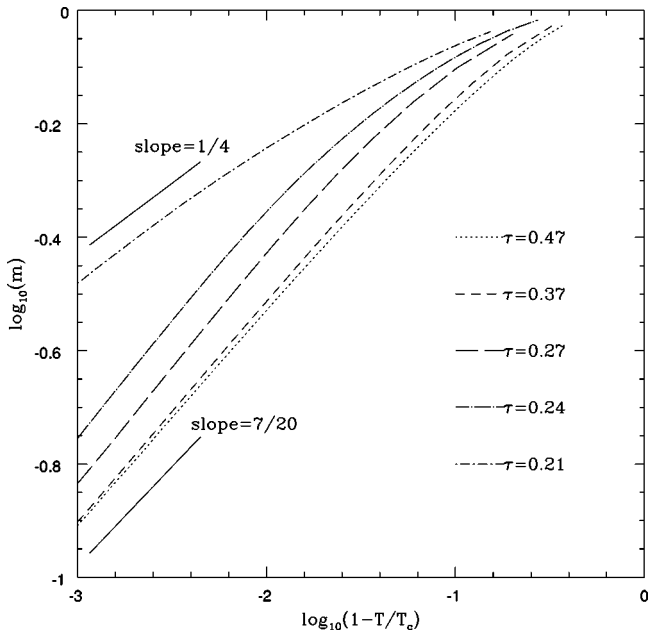

FIG. 10. Log-log plot of the order parameter m as a function of the reduced temperature $1-T/T_c$ in the second-order and tricritical regions.

asymptotic exponent $\beta_t=1/4$ for $\tau=\tau_t$.

Finally, we analyze the shape of the wing critical boundary as it approaches the TCP. Figure 11 shows the log-log plots of the critical field h_c and the magnetization m_c as a function of the reduced temperature $1-T_c/T_t$. Our numerical data are consistent with asymptotic power-law behaviors governed by the exponents 5/2 for h_c and 1/2 for m_c.

All the above numerical results strongly suggest that our theory describes the whole critical portion of the phase

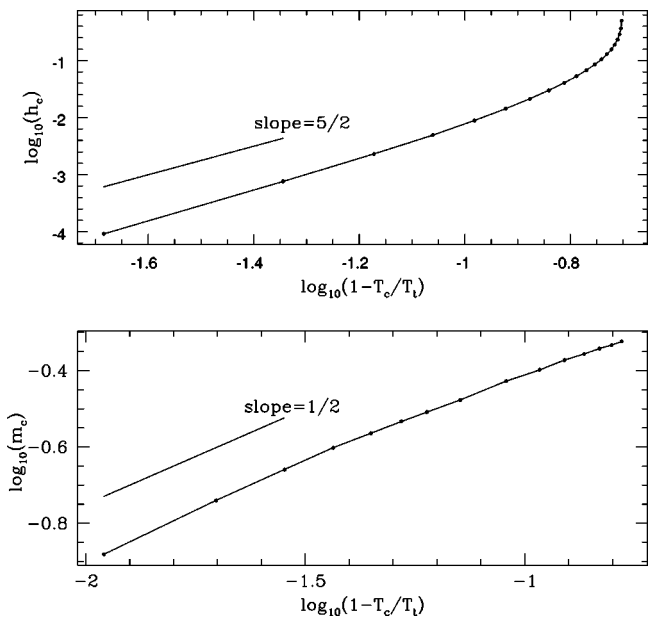

FIG. 11. Behavior of the wing boundaries as the TCP is approached; log-log plots of the critical field h_c and magnetization m_c as a function of the reduced temperature $1-T_c/T_t$.

boundary by the same exponents as the SCOZA equation for the spin-$\frac{1}{2}$ Ising model [2,3] and that near the TCP there is a crossover to a tricritical behavior described by mean-field exponents. This is supported, and can be further rationalized, by considering a heuristic scaling analysis of the coupled SCOZA PDE's, Eqs. (16). The argument is summarized below and detailed in Appendix B.

Let us assume that close to the TCP, the singular part of the Gibbs free energy can be written as

$$\mathcal{G}_{sing} \approx |t|^{2-\alpha} \mathcal{G}_{\pm}\left(\frac{g}{|t|^{\phi}}, \frac{m}{|t|^{\beta}}\right) \tag{24a}$$

$$\approx |g|^{2-\alpha_t} \mathcal{G}^{t}_{\pm}\left(\frac{t}{|g|^{\phi_t}}, \frac{m}{|g|^{\beta_t}}\right), \tag{24b}$$

where we have introduced the two scaling fields $t=(T-T_t)/T_t$ and $g=(\tau-\tau_t)/\tau_t - at$ where $(\tau_t/T_t)a = \partial\tau_\lambda/\partial T|_{T_t} > 0$ is the slope of the λ line at the TCP (this is also the slope of the triple line below T_t, as we have seen that the slope of the phase boundary is finite and continuous at the TCP). Equations (24) have the form of the standard tricritical scaling hypothesis [9,10], except that we use the magnetization m instead of the magnetic field h as variable. $\mathcal{G}_{(\pm)}$ and $\mathcal{G}^{t}_{(\pm)}$ are the scaling functions, where the subscript $(\pm)$ represents the sign of t, i.e., denotes when the temperature is above or below the tricritical temperature T_t. When $|t| \to 0$ with $g=0$, the TCP is approached tangentially to the phase boundary in the symmetry plane $h=0$ [and Eq. (24a) is then the convenient form of the scaling hypothesis], whereas the TCP is approached with a finite angle with the phase boundary when $g \neq 0$ [and Eq. (24b) is the convenient scaling form]. This defines two sets of exponents (α, ϕ, β) and $(\alpha_t, \phi_t, \beta_t)$ that are related through $2-\alpha_t = (2-\alpha)/\phi$, $\phi_t = 1/\phi$ and $\beta_t = \beta/\phi$.

Since SCOZA is thermodynamically self-consistent, the scaling behavior of the Gibbs free energy near the TCP is inherited by its various derivatives. In particular, the asymptotic behavior of the magnetic field $h=\partial(\mathcal{G}/N)/\partial m$ is

$$h \approx |t|^{2-\alpha-\beta} \frac{\partial}{\partial v} \mathcal{G}_{\pm}(u,v) \approx |g|^{2-\alpha_t-\beta_t} \frac{\partial}{\partial v_t} \mathcal{G}^{t}_{\pm}(u_t, v_t), \tag{25}$$

where $u = g/|t|^{\phi}$, $v = m/|t|^{\beta}$ $(u_t = t/|g|^{\phi_t}$, $v_t = m/|g|^{\beta_t})$, and the inverse ordering susceptibility $\chi_0^{-1} = \partial^2(\mathcal{G}/N)/\partial m^2$ and the singular part of the ^{4}He concentration order parameter $\rho = 1-x = \partial(\mathcal{G}/N)/\partial\Delta$ obey (up to irrelevant multiplying factors)

$$\chi_0^{-1} \approx |t|^{\gamma} \frac{\partial^2}{\partial v^2} \mathcal{G}_{\pm}(u,v) \approx |g|^{\gamma_t} \frac{\partial^2}{\partial v_t^2} \mathcal{G}^{t}_{\pm}(u_t, v_t) \tag{26}$$

and

$$\rho_{sing} \approx -|t|^{2-\alpha-\phi} \frac{\partial}{\partial u} \mathcal{G}_{\pm}(u,v)$$

$$\approx -|g|^{2-\alpha_t-\phi_t} \frac{\partial}{\partial u_t} \mathcal{G}^{t}_{\pm}(u_t, v_t), \tag{27}$$

where $\gamma = 2-\alpha-2\beta$ (respectively, $\gamma_t = 2-\alpha_t-2\beta_t$). Note also that because m is used in Eqs. (24) instead of h, the zero-field magnetization is solution of the implicit equation $h=\partial(\mathcal{G}/N)/\partial m = 0$. This implies that the singular part of this quantity near the TCP obeys $m_{sing} \approx |t|^{\beta} \mathcal{M}_{\pm}(g/|t|^{\phi}) \approx |g|^{\beta_t} \mathcal{M}^{t}_{\pm}(g/|t|^{\phi_t})$.

From the numerical results shown in Figs. (8)–(11), it appears that $\gamma_t \approx 1$ (see the curve $\tau = 0.22$ in the lower part of Fig. 8), $\beta_t \approx 1/4$ (see the curve $\tau = 0.21$ in Fig. 10), $2-\alpha-\beta \approx 5/2$, and $\beta \approx 1/2$ (upper and lower parts of Fig. 11). [We have also good numerical evidence that $\beta \approx 1/2$ from a log-log plot of the discontinuity of the zero-field magnetization as a function of $(T_t-T)/T_t$ across the first-order phase boundary.] All these exponents have their classical values, and from the scaling relation $\alpha+2\beta+\gamma=2$ (respectively, $\alpha_t+2\beta_t+\gamma_t=2$), we deduce that $\gamma=2$ and $\alpha_t=\frac{1}{2}$. These values are all consistent with a crossover exponent $\phi=2$.

We show in Appendix B that the scaling ansatz, Eqs. (24) or Eqs. (26)–(27), is compatible with the asymptotic behavior of the PDE's, Eqs. (16), in the tricritical region. This analysis indicates that a nontrivial scaling is found when the exponents obey the two relations $\gamma=\phi$ and $\gamma=4\beta$, which are satisfied by the classical values. Moreover, one finds that the scaling function of the zero-field susceptibility above T_t obeys an equation that is similar to the asymptotic SCOZA equation studied in Ref. [3] for the spin-$\frac{1}{2}$ model. It can be inferred that the critical behavior of the present theory along the λ line is the same as the SCOZA prediction for the Ising model. This is consistent with the exponent $\dot{\beta} = 7/20$, which is observed numerically in Fig. 9 along the high-temperature part of the λ line. This universality appears to hold along the wing critical lines too since the boundary condition to Eqs. (16) at the end of these lines (for $h_c \to \pm\infty$) is again the SCOZA PDE for the Ising model, as explained in Sec. II.

V. CONCLUSION

The present paper shows that a thermodynamically self-consistent OZ approximation provides a very good description of the properties of the 3D Blume-Capel model in all parts of the phase diagram. As in the case of the Ising model, nonuniversal properties such as the shape of the phase boundaries and the location of the tricritical point are predicted with remarkable accuracy. Moreover, there is good numerical and analytical evidence that the SCOZA correctly predicts a universal critical behavior along the λ line and the wing critical lines (with a zero-field magnetization exponent 0.35 that is very close to the true Ising value), as well as a crossover to tricritical behavior governed by classical exponents. Therefore, the SCOZA proves to be a powerful tool for studying spin systems that exhibit first-order and/or continuous transitions. This is confirmed by further work on the ferromagnetic spin-3/2 [20] and Potts [21] models.

APPENDIX A

In this Appendix, we derive the SCOZA equations for the most general spin-1 Hamiltonian with n.n. couplings,

$$\mathcal{H}=\mathcal{H}_{BC}-K\sum_{\langle ij\rangle} S_i^2S_j^2-L\sum_{\langle ij\rangle} S_iS_j(S_i+S_j), \qquad \text{(A1)}$$

which is a model for ternary mixtures [16]. The solution of these equations also provides a complete description of the pair correlation functions of the Blume-Capel model. These functions can be generated by introducing site-dependent fields h_i and Δ_i in the Hamiltonian (A1), which yields

$$G_{ij}^{SS}=\langle S_iS_j\rangle-\langle S_i\rangle\langle S_j\rangle=-\frac{\partial^2\tilde{\mathcal{F}}}{\partial\tilde{h}_i\partial\tilde{h}_j}, \qquad \text{(A2a)}$$

$$G_{ij}^{SS^2}=\langle S_iS_j^2\rangle-\langle S_i\rangle\langle S_j^2\rangle=\frac{\partial^2\tilde{\mathcal{F}}}{\partial\tilde{h}_i\partial\tilde{\Delta}_j}, \qquad \text{(A2b)}$$

$$G_{ij}^{S^2S^2}=\langle S_i^2S_j^2\rangle-\langle S_i^2\rangle\langle S_j^2\rangle=-\frac{\partial^2\tilde{\mathcal{F}}}{\partial\tilde{\Delta}_i\partial\tilde{\Delta}_j}. \qquad \text{(A2c)}$$

We then perform a double Legendre transform that takes the fields h_i and Δ_i into m_i and x_i, respectively, where $x_i=1-\langle S_i^2\rangle=1-\partial\mathcal{F}/\partial\Delta_i$. This defines a Gibbs free energy $\mathcal{G}(T,\{m_i\},\{x_i\})=\mathcal{F}+\Sigma_ih_im_i-\Sigma_i\Delta_i(1-x_i)$, which satisfies $h_i=\partial\mathcal{G}/\partial m_i$ and $\Delta_i=\partial\mathcal{G}/\partial x_i$. $\mathcal{G}$ is the generating functional of the direct correlation functions,

$$C_{ij}^{SS}=\frac{\partial^2\tilde{\mathcal{G}}}{\partial m_i\partial m_j}, \qquad \text{(A3a)}$$

$$C_{ij}^{SS^2}=-\frac{\partial^2\tilde{\mathcal{G}}}{\partial m_i\partial x_j}, \qquad \text{(A3b)}$$

$$C_{ij}^{S^2S^2}=\frac{\partial^2\tilde{\mathcal{G}}}{\partial x_i\partial x_j}, \qquad \text{(A3c)}$$

that are related to the G's via a set of Ornstein-Zernike equations. In the limit of uniform fields, these equations in Fourier space take the form $\hat{\underline{\mathbf{C}}}(\mathbf{k})\hat{\underline{\mathbf{G}}}(\mathbf{k})=1$, where $\hat{\underline{\mathbf{G}}}(\mathbf{k})$ and $\hat{\underline{\mathbf{C}}}(\mathbf{k})$ are symmetrical square matrices. This readily yields

$$\hat{G}^{SS}(\mathbf{k})=\frac{\hat{C}^{S^2S^2}(\mathbf{k})}{\hat{C}^{S^2S^2}(\mathbf{k})\hat{C}^{SS}(\mathbf{k})-\hat{C}^{SS^2}(\mathbf{k})^2}, \qquad \text{(A4a)}$$

$$\hat{G}^{S^2S^2}(\mathbf{k})=\frac{\hat{C}^{SS}(\mathbf{k})}{\hat{C}^{S^2S^2}(\mathbf{k})\hat{C}^{SS}(\mathbf{k})-\hat{C}^{SS^2}(\mathbf{k})^2}, \qquad \text{(A4b)}$$

$$\hat{G}^{SS^2}(\mathbf{k})=\frac{-\hat{C}^{SS^2}(\mathbf{k})}{\hat{C}^{S^2S^2}(\mathbf{k})\hat{C}^{SS}(\mathbf{k})-\hat{C}^{SS^2}(\mathbf{k})^2}. \qquad \text{(A4c)}$$

We now assume that the range of the direct correlation functions is limited to n.n. separation, i.e.,

$$\hat{C}^{SS}(\mathbf{k})=c_0^{SS}[1-\zeta_{SS}\hat{\lambda}(\mathbf{k})], \qquad \text{(A5a)}$$

$$\hat{C}^{SS^2}(\mathbf{k})=c_0^{SS^2}[1-\zeta_{SS^2}\hat{\lambda}(\mathbf{k})], \qquad \text{(A5b)}$$

$$\hat{C}^{S^2S^2}(\mathbf{k})=c_0^{S^2S^2}[1-\zeta_{S^2S^2}\hat{\lambda}(\mathbf{k})], \qquad \text{(A5c)}$$

where the c_0's and the ζ's are functions of T,m, and x to be determined. This fixes the form of the correlation functions in $\mathbf{r}$ space, and after some calculations we find

$$G^{SS}(\mathbf{r})=G^{SS}(\mathbf{r}=\mathbf{0})\times\frac{(z_1-\zeta_{S^2S^2})P(z_1,\mathbf{r})-(z_2-\zeta_{S^2S^2})P(z_2,\mathbf{r})}{(z_1-\zeta_{S^2S^2})P(z_1)-(z_2-\zeta_{S^2S^2})P(z_2)}, \qquad \text{(A6a)}$$

$$G^{SS^2}(\mathbf{r})=G^{SS^2}(\mathbf{r}=\mathbf{0})\times\frac{(z_1-\zeta_{SS^2})P(z_1,\mathbf{r})-(z_2-\zeta_{SS^2})P(z_2,\mathbf{r})}{(z_1-\zeta_{SS^2})P(z_1)-(z_2-\zeta_{SS^2})P(z_2)}, \qquad \text{(A6b)}$$

$$G^{S^2S^2}(\mathbf{r})=G^{S^2S^2}(\mathbf{r}=\mathbf{0})\times\frac{(z_1-\zeta_{SS})P(z_1,\mathbf{r})-(z_2-\zeta_{SS})P(z_2,\mathbf{r})}{(z_1-\zeta_{SS})P(z_1)-(z_2-\zeta_{SS})P(z_2)}, \qquad \text{(A6c)}$$

where $P(z,\mathbf{r})$ is the lattice Green's function defined by Eq. (10), and z_1,z_2 are related to the c_0's and the ζ's via the relations

$$\zeta_{SS}+\zeta_{S^2S^2}=2R^2\zeta_{SS^2}+(1-R^2)(z_1+z_2), \qquad \text{(A7a)}$$

$$\zeta_{SS}\zeta_{S^2S^2}=R^2\zeta_{SS^2}^2+(1-R^2)z_1z_2, \qquad \text{(A7b)}$$

and

$$\frac{R}{R_0}=\frac{\{z_1P(z_1)-z_2P(z_2)-\zeta_{SS}[P(z_1)-P(z_2)]\}^{1/2}\{z_1P(z_1)-z_2P(z_2)-\zeta_{S^2S^2}[P(z_1)-P(z_2)]\}^{1/2}}{z_1P(z_1)-z_2P(z_2)-\zeta_{SS^2}[P(z_1)-P(z_2)]}, \qquad \text{(A8)}$$

where $R=c_0^{SS^2}/(c_0^{SS}c_0^{S^2S^2})^{1/2}$ and R_0 is the high-temperature limit of R, which can be calculated exactly, as explained below. Note that in Eqs. (A6) we have eliminated the c_0's to introduce the on-site values of the correlation functions that are simple functions of the order parameters m and x. Indeed, since S_i can only take the values $0,\pm 1$, one has $\langle S_i^3\rangle=\langle S_i\rangle$ and $\langle S_i^4\rangle=\langle S_i^2\rangle$, so that

$$G^{SS}(\mathbf{r}=\mathbf{0})=1-x-m^2, \tag{A9a}$$

$$G^{SS^2}(\mathbf{r}=\mathbf{0})=mx, \tag{A9b}$$

$$G^{S^2S^2}(\mathbf{r}=\mathbf{0})=x(1-x). \tag{A9c}$$

In terms of these variables, one also has

$$\hat{C}^{SS}(\mathbf{k}=\mathbf{0})=\frac{1-\zeta_{SS}}{(1-R^2)(1-x-m^2)}\,\frac{z_1P(z_1)-z_2P(z_2)-\zeta_{S^2S^2}[P(z_1)-P(z_2)]}{z_1-z_2}, \tag{A10a}$$

$$\hat{C}^{SS^2}(\mathbf{k}=\mathbf{0})=-\frac{(1-\zeta_{SS^2})R^2}{(1-R^2)xm}\,\frac{z_1P(z_1)-z_2P(z_2)-\zeta_{SS^2}[P(z_1)-P(z_2)]}{z_1-z_2}, \tag{A10b}$$

$$\hat{C}^{S^2S^2}(\mathbf{k}=\mathbf{0})=\frac{1-\zeta_{S^2S^2}}{(1-R^2)x(1-x)}\,\frac{z_1P(z_1)-z_2P(z_2)-\zeta_{SS}[P(z_1)-P(z_2)]}{z_1-z_2}. \tag{A10c}$$

Three unknown functions remain to be determined, and it is convenient to choose z_1,z_2, and R and to use Eqs. (A7) and (A8) to calculate the ζ's. The three additional equations that we need are obtained by imposing thermodynamic self-consistency. On the one hand, the enthalpy is given by

$$\frac{\partial\tilde{\mathcal{G}}/N}{\partial\beta}=-\frac{Jc}{2}[G^{SS}(\mathbf{r}=\mathbf{e})+m^2]-\frac{Kc}{2}[G^{S^2S^2}(\mathbf{r}=\mathbf{e})+(1-x)^2]-Lc[G^{SS^2}(\mathbf{r}=\mathbf{e})+m(1-x)]. \tag{A11}$$

On the other hand, we have from Eqs. (A3)

$$\hat{C}^{SS}(\mathbf{k}=\mathbf{0})=\frac{\partial^2\tilde{\mathcal{G}}}{\partial m^2}, \tag{A12a}$$

$$\hat{C}^{SS^2}(\mathbf{k}=\mathbf{0})=-\frac{\partial^2\tilde{\mathcal{G}}}{\partial m\,\partial x}, \tag{A12b}$$

$$\hat{C}^{S^2S^2}(\mathbf{k}=\mathbf{0})=\frac{\partial^2\tilde{\mathcal{G}}}{\partial x^2}. \tag{A12c}$$

This yields the three Maxwell equations

$$\frac{\partial\hat{C}^{SS}(\mathbf{k}=\mathbf{0})}{\partial\lambda}=-1-\frac{1}{2}\,\frac{\partial^2[G^{SS}(\mathbf{r}=\mathbf{e})+\alpha_1G^{S^2S^2}(\mathbf{r}=\mathbf{e})+2\alpha_2G^{SS^2}(\mathbf{r}=\mathbf{e})]}{\partial m^2}, \tag{A13a}$$

$$\frac{\partial\hat{C}^{SS^2}(\mathbf{k}=\mathbf{0})}{\partial\lambda}=-\alpha_2+\frac{1}{2}\,\frac{\partial^2[G^{SS}(\mathbf{r}=\mathbf{e})+\alpha_1G^{S^2S^2}(\mathbf{r}=\mathbf{e})+2\alpha_2G^{SS^2}(\mathbf{r}=\mathbf{e})]}{\partial m\,\partial x}, \tag{A13b}$$

$$\frac{\partial\hat{C}^{S^2S^2}(\mathbf{k}=\mathbf{0})}{\partial\lambda}=-\alpha_1-\frac{1}{2}\,\frac{\partial^2[G^{SS}(\mathbf{r}=\mathbf{e})+\alpha_1G^{S^2S^2}(\mathbf{r}=\mathbf{e})+2\alpha_2G^{SS^2}(\mathbf{r}=\mathbf{e})]}{\partial x^2}, \tag{A13c}$$

where $\lambda=\beta Jc$, $\alpha_1=K/J$, and $\alpha_2=L/J$.

These equations, together with Eqs. (A7) and (A8), constitute a set of three PDE's in the unknown functions $z_1(\lambda,m,x)$, $z_2(\lambda,m,x)$, and $R(\lambda,m,x)$, whose solution encodes the full thermodynamics of the model Hamiltonian (A1). The initial conditions for $J=K=L=0$ are easily obtained since the correlation functions are then nonzero at $\mathbf{r}=\mathbf{0}$ only. One has $z_1=z_2=0$ and from Eqs. (A4) and (A9)

$$R_0 = -\frac{mx}{[x(1-x)(1-x-m^2)]^{1/2}}. \tag{A14}$$

It should be noticed that in the case of the Blume-Capel model (for which $\alpha_1=\alpha_2=0$), this SCOZA is different from the one presented in the main text. This can checked for instance by computing the high-temperature expansion of the solution. Both theories yield zero-field properties that are exact through order λ^4. It is unclear which one provides the best numerical predictions.

APPENDIX B

In this appendix, we show that the tricritical scaling hypothesis, Eqs. (24) or (26)–(27), is consistent with the asymptotic behavior of the SCOZA PDE's, Eqs. (16). The notations are those of the main text.

To this end, it is convenient to rewrite the PDE's in terms of the two variables $\mathcal{E}=(1-z)^{1/2}$ and $\rho=1-x$. $\mathcal{E}^2$ is proportional to the inverse susceptibility χ_0^{-1} and $\rho=G(\mathbf{r}=\mathbf{0})+m^2=P(z)/c_0+m^2$. At the TCP, we have $\mathcal{E}=0$ and $\rho=\rho_t$. For $t\to 0$, $m\to 0$, and $\rho\to\rho_t$, Eqs. (16) take the asymptotic form

$$\frac{P(1)^2}{\rho_t\lambda_t}\frac{\partial\mathcal{E}^2}{\partial t} = 1-\left(\frac{P(1)-1}{2}\right)\left[\frac{b\rho_t}{P(1)-1}\frac{\partial^2\mathcal{E}}{\partial m^2}-\frac{\partial^2\rho}{\partial m^2}\right], \tag{B1a}$$

$$\frac{\partial\rho}{\partial t} = \frac{1}{2}\lambda_t(1-\tau_t)\frac{P(1)-1}{P(1)}\left[\frac{b\rho_t}{P(1)-1}\frac{\partial\mathcal{E}}{\partial\delta\tau}-\frac{\partial\rho}{\partial\delta\tau}\right], \tag{B1b}$$

where $t=(T-T_t)/T_t$, $\lambda_t=cJ/(k_BT_t)$, $\delta\tau=(\tau-\tau_t)/\tau_t$, and we have used the expansion of the 3D lattice Green function for $z\to 1$, $P(z)\sim P(1)[1-b\mathcal{E}+O(\mathcal{E}^2)]$, where b is a positive constant [22]. In these equations and in the following, all derivatives are taken at the TCP.

By suitably rescaling the variables as $\mathcal{E}\to b\rho_t/[P(1)-1]\mathcal{E}$, $t\to\lambda_t b^2\rho_t^3/[P(1)(P(1)-1)]^2 t$, $m\to m/[P(1)-1]^{1/2}$, and $\delta\tau\to b^2\rho_t^3/\{P(1)[P(1)-1]^3(1-\tau_t)\}\delta\tau$, we obtain the two simplified equations

$$\frac{\partial\mathcal{E}^2}{\partial t} = 1-\frac{1}{2}\frac{\partial^2(\mathcal{E}-\rho)}{\partial m^2}, \tag{B2a}$$

$$\frac{\partial\rho}{\partial t} = \frac{1}{2}\frac{\partial(\mathcal{E}-\rho)}{\partial\delta\tau}. \tag{B2b}$$

We now introduce the tricritical scaling ansatz for $\mathcal{E}$ and for the singular part of ρ, according to Eqs. (26) and (27),

$$\mathcal{E}\approx|t|^{\gamma/2}E_\pm(u,v), \tag{B3}$$

$$\rho_{sing}\approx|t|^{2-\alpha-\phi}R_\pm(u,v), \tag{B4}$$

where $u=g/|t|^\phi$ and $v=m/|t|^\beta$. Because of thermodynamic self-consistency, $E_\pm$ and $R_\pm$ obey

$$\frac{\partial E_\pm^2}{\partial u} = -\frac{\partial^2 R_\pm}{\partial v^2}. \tag{B5}$$

For the sake of simplicity, we only consider the case $t>0$ (i.e., $T>T_t$), but a similar analysis can be performed for $t<0$. Then Eqs. (B2) yield

$$t^{\gamma-1}\left[\gamma E_+^2-\phi u\frac{\partial E_+^2}{\partial u}-\beta v\frac{\partial E_+^2}{\partial v}\right]+a(\phi-1)t^{\gamma-\phi}\frac{\partial E_+^2}{\partial u} = 1-\frac{1}{2}\left[t^{\gamma/2-2\beta}\frac{\partial^2 E_+}{\partial v^2}-t^{\gamma-\phi}\frac{\partial^2 R_+}{\partial v^2}\right], \tag{B6a}$$

$$t^{1-\alpha}\left[(2-\alpha-\phi)R_+-\phi u\frac{\partial R_+}{\partial u}-\beta v\frac{\partial R_+}{\partial v}\right] + a(\phi-1)t^{2-\alpha-\phi}\frac{\partial R_+}{\partial u} = \frac{1}{2}\left[t^{\gamma/2}\frac{\partial E_+}{\partial u}-t^{2-\alpha-\phi}\frac{\partial R_+}{\partial u}\right], \tag{B6b}$$

where we have used the scaling relation $\gamma=2-\alpha-2\beta$, which results from thermodynamic self-consistency. If the crossover exponent ϕ is greater than 1 (which is usually the case and is indeed found numerically), the first term in the left-hand side of Eq. (B6a) may be neglected asymptotically. A nontrivial scaling is then found when the exponents are related through the two relations $\gamma=\phi=4\beta$. For the same reason we may neglect the first term in the left-hand side of Eq. (B6b) and we obtain the relation $\gamma=2(2-\alpha-\phi)$ (which is not independent from the preceding ones). Actually, we expect that as in the SCOZA for the Ising model, the enthalpy is analytic in m^2 and $T-T_c$ when approaching a critical point from a disordered phase, which corresponds to $\gamma=2$ and $\beta=1/2$. (At the tricritical point, the m^2 term of course vanishes.) The scaling functions satisfy the two nontrivial PDE's

$$a(\phi-1)\frac{\partial E_+^2}{\partial u} = 1-\frac{1}{2}\frac{\partial^2(E_+-R_+)}{\partial v^2}, \tag{B7a}$$

$$\frac{\partial E_+}{\partial u} = [1+2a(\phi-1)]\frac{\partial R_+}{\partial u}. \tag{B7b}$$

Using Eq. (B5) to eliminate one of the functions, we finally obtain a single equation for E_+

$$\frac{\partial E_+^2}{\partial u} = 1-\frac{1}{2}\frac{\partial^2 E_+}{\partial v^2}, \tag{B8}$$

where we have used the rescaling $u\to 2/[2a(\phi-1)+1]u$. (Note that the multiplying factor is positive since $a>0$ and $\phi>1$.) Of course, this equation must be accompanied by some boundary conditions. These are obtained from the analytical requirements that the scaling functions must satisfy near the TCP and in the vicinity of the critical lines and the coexistence surfaces (see, e.g., Ref. [10]). It can be shown that these boundary conditions are also compatible with the

SCOZA equations. The other function R_+ can be obtained as $[1+2a(\phi-1)]R_+(u,v)=E_+(u,v)-v^2+R_{+0}$, where R_{+0} is a constant that can be determined by the boundary conditions.

Equation (B8) has an important consequence for the scaling behavior near the TCP when one approaches the λ line along a path at fixed τ. The convenient temperature variable is then $\dot{t}=[T-T_\lambda(\tau)]/T_t$, which measures the distance from λ line at fixed τ, so that $t=\dot{t}+t_\lambda$, where $t_\lambda=[T_\lambda(\tau)-T_t]/T_t$ defines the λ line near the TCP. When $|\dot{t}|\to 0$, or $t\to t_\lambda(\tau)$, the scaling field g behaves as $g-g_0\sim\dot{t}$, where $g_0=(\tau-\tau_t)/\tau_t$ is a constant, and the scaling variables u and v behave as $u-u_0\sim\dot{t}$ and $v\sim m$, where u_0 is a constant. As a consequence, Eq. (B8) can be rewritten as

$$\frac{\partial E_+^2}{\partial \dot{t}}=1-\frac{1}{2}\frac{\partial^2 E_+}{\partial m^2}. \tag{B9}$$

This is precisely the asymptotic SCOZA equation for the spin-$\frac{1}{2}$ Ising model that has been studied in Ref. [3] (with E_+ playing the role of the variable ϕ in that reference). Therefore, one expects that the critical behavior above and below the critical temperature $T_\lambda(\tau)$ will be identical to that of the SCOZA for the Ising model [with for instance $\dot{\beta}=7/20$ for the zero-field magnetization $m(\dot{t})$].

[1] J. S. Hoye and G. Stell, J. Chem. Phys. **67**, 439 (1977); Mol. Phys. **52**, 1071 (1984); Int. J. Thermophys. **6**, 561 (1985).

[2] R. Dickman and G. Stell, Phys. Rev. Lett. **77**, 996 (1996); D. Pini, G. Stell, and R. Dickman, Phys. Rev. E **57**, 2862 (1998).

[3] J. S. Hoye, D. Pini, and G. Stell, Physica A **279**, 213 (2000).

[4] J. S. Hoye and G. Stell, Physica A **244**, 176 (1997); **247**, 497 (1997).

[5] D. Pini, G. Stell, and N. B. Wilding, Mol. Phys. **95**, 483 (1998).

[6] E. Kierlik, M. L. Rosinberg, and G. Tarjus, J. Stat. Phys. **89**, 215 (1997); **94**, 805 (1999); **100**, 423 (2000).

[7] M. Blume, Phys. Rev. **141**, 517 (1966); H. W. Capel, Physica **32**, 966 (1966).

[8] M. Blume, V. J. Emery, and R. B. Griffiths, Phys. Rev. A **4**, 1071 (1971).

[9] E. K. Riedel and F. J. Wegner, Phys. Rev. Lett. **29**, 349 (1972); F. J. Wegner and E. K. Riedel, Phys. Rev. B **7**, 248 (1973); E. K. Riedel and F. J. Wegner, *ibid.* **9**, 294 (1974).

[10] I. D. Lawrie and S. Sarbach, in *Phase Transitions and Critical Phenomena*, edited by C. Domb and J. L. Lebowitz (Academic, London, 1984), Vol. 9.

[11] P. F. Fox and D. S. Gaunt, J. Phys. C **5**, 3085 (1972); J. Oitmaa, *ibid.* **5**, 435 (1972); D. M. Saul, M. Wortis, and D. Stauffer, Phys. Rev. B **9**, 4964 (1974).

[12] A. N. Berker and M. Wortis, Phys. Rev. B **14**, 4946 (1976); T. W. Burkhard *ibid.* **14**, 1196 (1976); T. W. Burkhardt and H. J. F. Knops, *ibid.* **15**, 1602 (1977); G. D. Mahan and S. M. Girvin, *ibid.* **17**, 4411 (1978); M. Kaufman, R. B. Griffiths, J. M. Yeomans, and M. E. Fisher, *ibid.* **23**, 3448 (1981); J. M. Yeomans and M. E. Fisher, *ibid.* **24**, 2825 (1981).

[13] B. L. Arora and D. P. Landau, AIP Conf. Proc. **10**, 870 (1973); A. K. Jain and D. P. Landau, Phys. Rev. B **22**, 445 (1980); W. Selke and J. Yeomans, J. Phys. A **16**, 2789 (1983); C. M. Care, *ibid.* **26**, 1481 (1993); M. Deserno, Phys. Rev. E **56**, 5204 (1997).

[14] J. S. Hoye and G. Stell, J. Stat. Phys. **89**, 177 (1997).

[15] S. Krinsky and D. Furman, Phys. Rev. B **11**, 2602 (1975).

[16] D. Mukamel and M. Blume, Phys. Rev. A **10**, 610 (1974).

[17] W. H. Press, B. P. Flannery, S. A. Teukolsky, and W. T. Vetterling, *Numerical Recipes* (Cambridge University Press, Cambridge, 1992).

[18] H. W. Blöte, E. Luijten, and J. R. Heringa, J. Phys. A **28**, 6289 (1995).

[19] J. R. Heringa and H. W. J. Blöte, Phys. Rev. E **57**, 4976 (1998).

[20] S. Grollau (unpublished).

[21] S. Grollau, M.L. Rosinberg, and G. Tarjus (unpublished).

[22] G. S. Joyce, in *Phase Transitions and Critical Phenomena*, edited by C. Domb and M. S. Green (Academic Press, London, 1972), Vol. 2, p. 375.